Electronic Supplementary Material (ESI) for Integrative Biology.

Chemical imaging of molecular changes in a hydrated single cell by dynamic secondary ion mass spectrometry and super-resolution microscopy

Xin Hua[1,3], Craig Szymanski[2,†], Zhaoying Wang[2,†], Yufan Zhou[2], Xiang Ma[4], Jiachao Yu[1,3], James Evans[2], Galya Orr[2], Songqin Liu[1,], Zihua Zhu[2,*], and Xiao-Ying Yu[3,*]*

[1]School of Chemistry and Chemical Engineering, Southeast University, Nanjing, Jiangsu Province, 211189 (China)

[2]W. R. Wiley Environmental Molecular Science Laboratory, Pacific Northwest National Laboratory, Richland, WA 99352 (USA)

[3]Earth and Biological Sciences Directorate, Pacific Northwest National Laboratory, Richland, WA 99354 (USA).

[4]Physical and Computational Sciences Directorate, Pacific Northwest National Laboratory, Richland, WA 99354 (USA).

Supplementary Figures

Additional experimental results including figures and tables are provided below. The following figures and tables are provided to substantiate the results and discussion section.

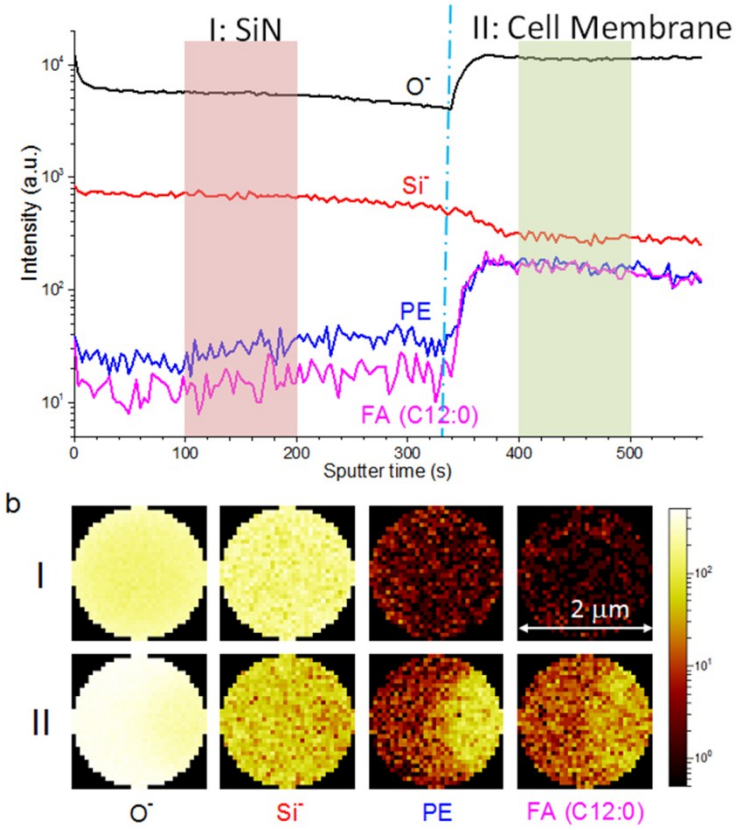

Figure S1. ToF-SIMS depth profiling and 2D imaging of C10 cell. (a) ToF-SIMS depth profile of a hydrated C10 cell in SALVI. Two time regions indicating different depths are highlighted and defined as I (100-200 s) or before SiN punch-through and II (400-500 s) or in the cell membrane. The blue dashed line indicates the beginning of SiN punch-through. (b) 2D ToF-SIMS images of O^- (m/z 16), Si^- (m/z 28), PE head group fragment (m/z 180), and fatty acid FA (C12:0) (m/z 199) reconstructed corresponding regions I and II in (a), respectively.

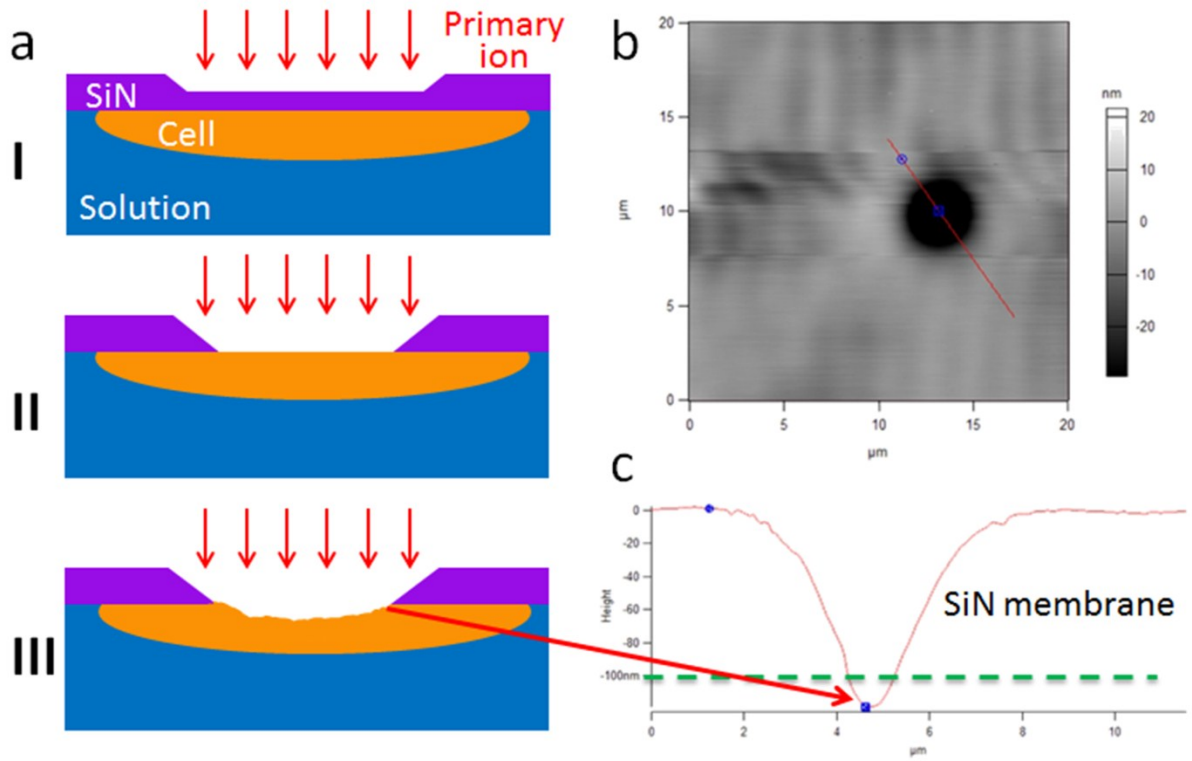

Figure S2. (a) Schematic illustration of ToF-SIMS detection of a single cell cultured in SALVI. **(b)** AFM image of the hole on SiN membrane with C10 cell attached drilled by ToF-SIMS. **(c)** AFM measurement of the hole in **(b)**. The depth of the hole is 121.4 nm.

Since our ToF-SIMS is not equipped with *in situ* tomography and depth measurement capabilities, correlative imaging with atomic force microscopy (AFM) was conducted to determine the crater depth in the cell (Figure S1) after SIMS measurements. The total depth of the hole, including the 100 nm thick SiN membrane and the depth of the crater into the cell, was determined to be 121.4 nm. It is known that the mammalian cell membrane thickness is below 4 nm in general.[1] The AFM measurement provided evidence that the cell membrane was actually being drilled through and the cell material was probed using the dynamic ToF-SIMS approach. These results are expected because after long depth profiling a crater would be produced in the cell materials. Unlike pure liquid, cells are soft materials. The cell membrane itself has complex structure and chemical composition. Many consider the cell membrane as a

fluid mosaic consisting of phospholipids, cholesterol, proteins, and carbohydrates. Our results seem to support this knowledge.

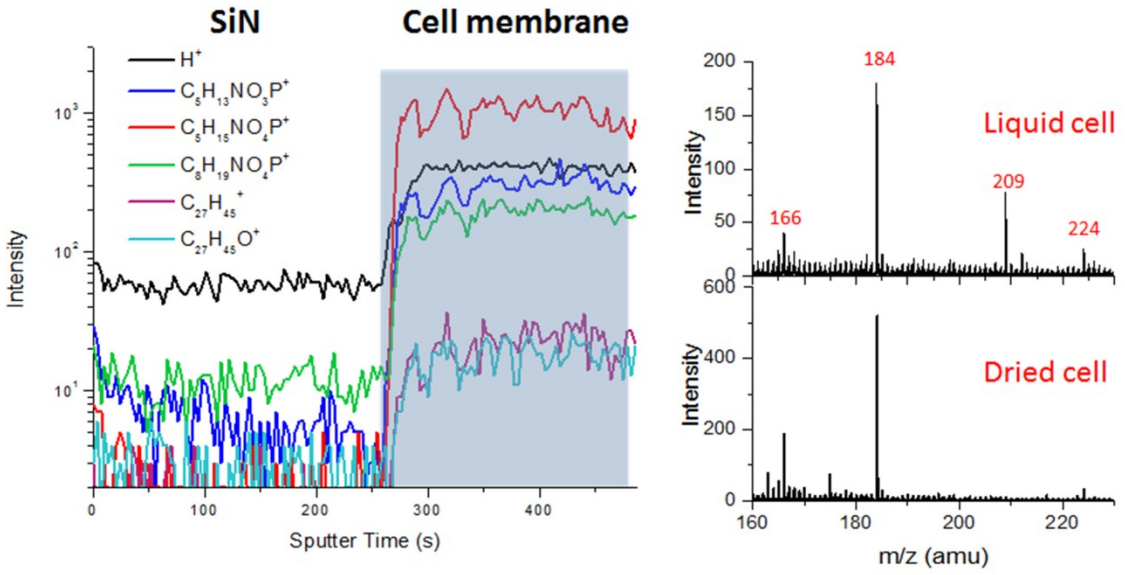

Figure S3a ToF-SIMS depth profiling of the hydrated C10 cell in the positive mode.

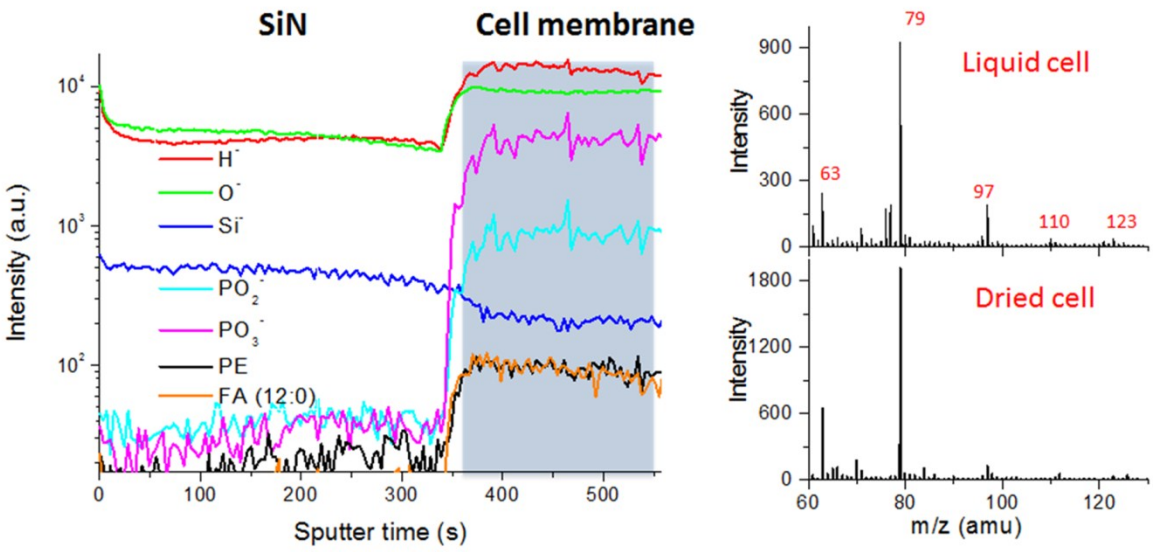

Figure S3b ToF-SIMS depth profiling of the hydrated C10 cell in the negative mode.

ToF-SIMS dynamic depth profiling data in the positive mode (Figure S3a) and negative mode (Figure S3b) are presented in addition to Fig. 3. The blue shaded region corresponds to the cell membrane after the SiN membrane was punched through. The m/z 209 peak is likely to be Bi^+ in the positive mode in Figure S2a. Other characteristic peaks known as phosphatidylcholine (PC) fragments (e.g., m/z 166, $C_5H_{13}NO_3P^+$, m/z 184, $C_5H_{15}NO_4P^+$) and cholesterol peaks (e.g., m/z 224, $C_8H_{19}NO_4P^+$, m/z 369, $C_{27}H_{45}^+$, m/z 385 $C_{27}H_{45}O^+$) are also observed. These observations provide strong evidence that the cell membrane was being drilled through. Additional peaks were provided in the negative mode depth profiling in Figure S3b.

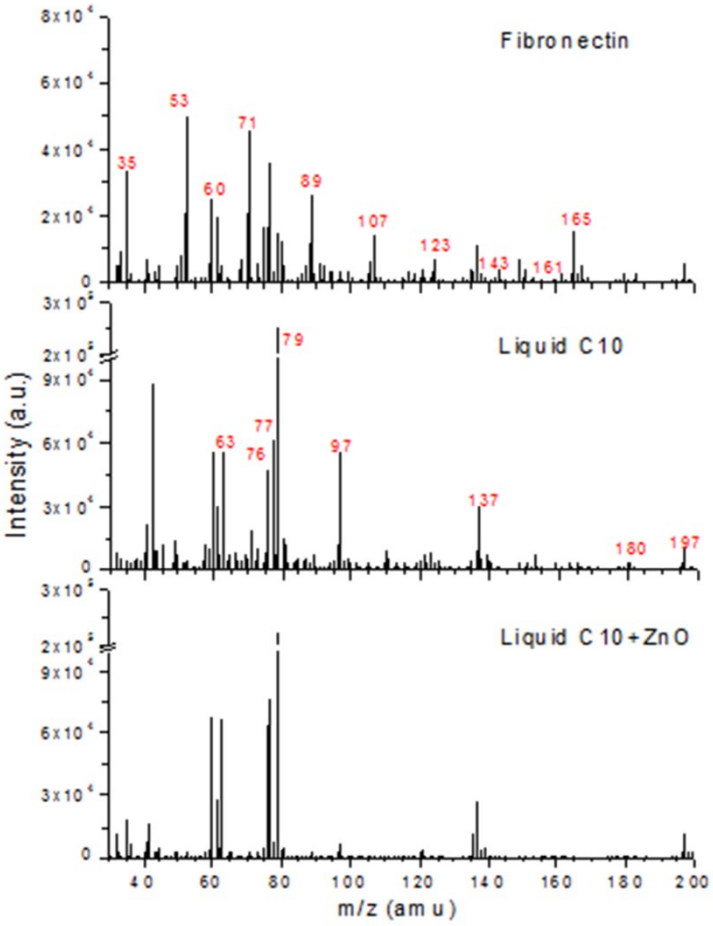

Figure S4. Negative ToF-SIMS spectra of fibronectin coated SiN-water interface, liquid C10 cell in SALVI and liquid C10 cells treated with ZnO NPs.

In addition, negative secondary ion spectra of the samples were presented in Figure S4 within the range of m/z 30-200 (see Table S3 for peak assignment). PO_2^- (m/z 63), PO_3^- (m/z 79) and $H_2PO_4^-$ (m/z 97) attributed from phospholipid fragments were observed in both the liquid C10 cell and ZnO NP treated C10 cell sample. In addition, many water cluster peaks were observed (i.e., OH^- m/z 17, $(H_2O)OH^-$ m/z 35, m/z 53 $(H_2O)_2OH^-$ m/z 53, $(H_2O)_3OH^-$ m/z 71, $(H_2O)_4OH^-$ m/z 89, $(H_2O)_5OH^-$ m/z 107, $(H_2O)_6OH^-$ m/z 125, m/z 143) in the fibronectin control and normal C10 cells compared to ZnO NP exposed C10 cells.

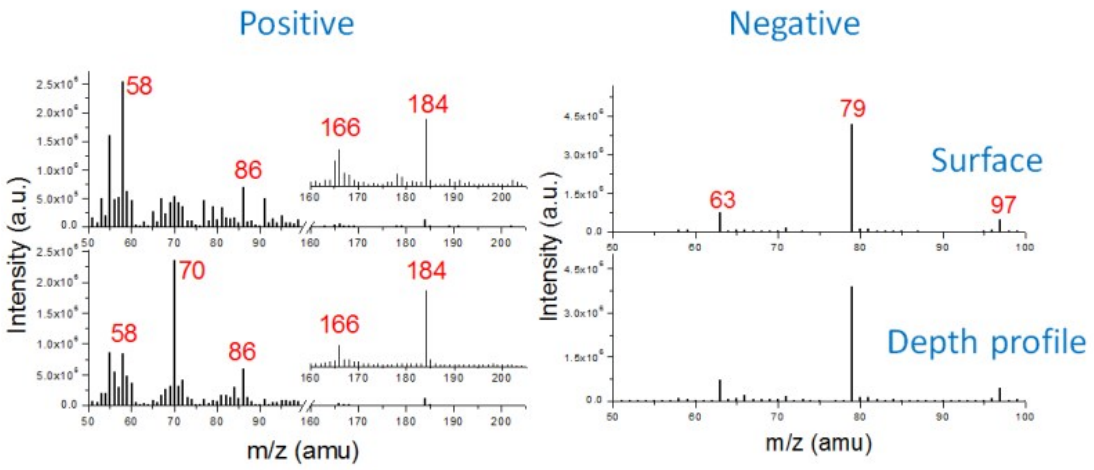

Figure S5. (a) ToF-SIMS positive spectra of surface and depth profiling of dried C10 cells. (b) ToF-SIMS negative spectra of surface and depth profiling of dried C10 cells, respectively.

As a comparison, both positive and negative spectra of dried cell surface and depth profiling were seen in Figure S5a and S5b. The depth profiling m/z spectrum of dried samples was obtained by using the Ar_n^+ cluster as the sputtering beam. Supplementary Fig. S5a showed the positive secondary ion spectra of the surface of a dried C10 cell and depth profiling of a dried C10 cell in the m/z range of 50-100 and 160-205. Negative spectra comparisons are seen in Supplementary Fig. S5b. The surface and depth profiling measurements of dry C10 samples showed some similarities. For example, m/z 166 and m/z 184 show similar trends in the cell surface and the depth profiling mass spectra. The case for m/z 70 is different, which is speculated to be an amino acid fragment that mainly exists in nucleus.[2] This peak is not as strong in the surface spectrum, reflecting the chemical difference in the surface and depth profiling of cell components. They provide additional evidence that we did observe the C10 characteristic fragments in the hydrated C10 cell analysis by in situ liquid ToF-SIMS.

Supplementary Tables

Peak assignments are a challenge in ToF-SIMS analysis. In the following, characteristic m/z fragments are assigned largely based on previous findings.[3]

For convenience of discussions, Table S1 is provided to accompany results in Fig. 2b.

Table S1. The negative peak assignment for Fig. 2b.

m/z	Assignment	Notes
97	$PO_4H_2^-$	PE/PC fragment
123	$C_2H_4NPO_3^-$	PE fragment
137	$Si_2O_5H^-$	SiN interference
165	$C_4H_8NPO_4^-$	PE fragment
180	$C_5H_{11}NPO_4^-$	PE head group
199	$C_{12}H_{23}O_2^-$	Fatty acid C12

For convenience of discussions, Table S2 is provided to accompany results in Fig. 4.

Table 2. The positive peak assignment for Fig. 4.

m/z	Assignment	Notes
28	Si^+/CO^+	
39	K^+	
55	$(H_2O)_3H^+$	Water cluster
58	$C_3H_8N^+$	PC fragment
70	$C_4H_8N^+$	Proline fragment
73	$(H_2O)_4H^+$	Water cluster
86	$C_5H_{12}N^+$	PC fragment
91	$(H_2O)_5H^+$	Water cluster
166	$C_5H_{13}NO_3P^+$	PC fragment
184	$C_5H_{15}NO_4P^+$	PC fragment

For convenience of discussions, Table 3 is provided to accompany results in Figure S4b.

Table 3. The negative peak assignment for Figure S4b.

m/z	Assignment	Notes
26	CN^-	
35	Cl^- or H_2OOH^-	Water cluster or chloride
42	CNO^-	
53	$(H_2O)_2OH^-$	Water cluster
60	SiO_2^-	
63	PO_2^-	PE fragment
71	$(H_2O)_3OH^-$	Water cluster
76	SiO_3^-	
77	SiO_3H^-	
79	PO_3^-	PE fragment
89	$(H_2O)_4OH^-$	Water cluster
97	$PO_4H_2^-$	PE fragment
107	$(H_2O)_5OH^-$	Water cluster
123	$C_2H_4NPO_3^-$	PE fragment
137	$Si_2O_5H^-$	SiN interference
143	$(H_2O)_6OH^-$	Water cluster
161	$(H_2O)_7OH^-$	Water cluster
165	$C_4H_8NPO_4^-$	PE fragment
180	$C_5H_{11}NO_4P^-$	PE fragment
199	$C_{12}H_{23}O_2^-$	Fatty acid C12

References

1. (a) K. Mitra, I. Ubarretxena-Belandia, T. Taguchi, G. Warren, D. M. Engelman, Modulation of the bilayer thickness of exocytic pathway membranes by membrane proteins rather than cholesterol. *Proceedings of the National Academy of Sciences* 2004, *101*. 4083-4088, DOI: 10.1073/pnas.0307332101; (b) O. S. Andersen, R. E. Koeppe, Bilayer Thickness and Membrane Protein Function: An Energetic Perspective. *Annual Review of Biophysics and Biomolecular Structure* 2007, *36*. 107-130, DOI: doi:10.1146/annurev.biophys.36.040306.132643.
2. D. Breitenstein, C. Rommel, R. Mollers, J. Wegener, B. Hagenhoff, The chemical composition of animal cells and their intracellular compartments reconstructed from 3D mass spectrometry. *Angew Chem Int Ed* 2007, *46*. 5332 - 5335.
3. (a) H. Tian, J. S. Fletcher, R. Thuret, A. Henderson, N. Papalopulu, J. C. Vickerman, N. P. Lockyer, Spatiotemporal lipid profiling during early embryo development of Xenopus laevis using dynamic ToF-SIMS imaging. *Journal of Lipid Research* 2014, *55*. 1970-1980, DOI: 10.1194/jlr.D048660; (b) M. K. Passarelli, N. Winograd, Lipid imaging with time-of-flight secondary ion mass spectrometry (ToF-SIMS). *Biochim. Biophys. Acta Mol. Cell Biol. Lipids* 2011, *1811*. 976-990, DOI: 10.1016/j.bbalip.2011.05.007.